Electronic Supplementary Information

Growth of Two-dimensional Formamidine Lead Halide Perovskites Single-crystalline Sheets and Their Optoelectronic Properties

Na Lu[a], Di Wang[a, b], Meina Han[a], Bojin Zho[a], Guozheng Wu[a], Zhanggui Hu*[a]*

[a] Institute of Functional Crystals, and Tianjin Key Laboratory of Functional Crystal Materials, Tianjin University of Technology, Tianjin 300384, China.

[b] Physics and Electronic Engineering School, Jiangsu Second Normal University, Nanjing 210013, China

E-mail: diwang@tjut.edu.cn Hu@mail.ipc.ac.cn

Experimental Procedures

Two-dimensional $FAPbX_3$ growth. 2D $FAPbX_3$ and $FAPbBr_{3-x}I_x$ single-crystalline sheets were grown on the fluorophlogopite mica substrate. The growth processes included two steps, the precursor solution preparation and 2D sheet growth, which were similar to our previous works.[1]

For the precursor solution preparation, formamidinium bromide (FABr, >99% Sigma-Aldrich), methylammonium bromide (MABr, >99% Sigma-Aldrich), and Lead(Ⅱ) bromide ($PbBr_2$, 99.999% Sigma-Aldrich) were mixed in the stoichiometry ratio of $MAPbBr_{3-x}I_x$ (x=0~3), and dissolved in a solution mixture of N,N-dimethylformamide (DMF, 99.5%-Sigma Aldrich) and γ-butyrolactone (GBL, 99.5%-Sigma Aldrich). The volume ratio of DMF : GBL was 1 : 1. The mixture was put under the nitrogen environment and stirred at 80℃ for 24h until tiny orange $FAPbBr_3$ crystals appeared. After that, the solution was filtered using a 0.3 μm pore-sized PTFE filter to remove the precipitations and obtained a clear precursor solution (1.0 M). Oleic acid (OA, >99% Sigma-Aldrich) was added into the prepared precursor solution in a volume ratio of 8 : 2 (solution : OA).

For 2D sheet growth, one fluorophlogopite mica (single crystals, Taiyuan) was cleaved into two pieces as the substrate and cover, respectively. The 50 μL precursor solution was dripped on the surface, then covered using the other mica. This growth system was fixed on the stage and spin at 3000 r.p.m. for the 30s under an N_2 environment. After that, the growth system was heated using the hot stage for 24h at 80℃, resulting in the growth of ultrathin 2D $FAPbBr_3$ single-crystalline sheets on the mica surfaces. Finally, the as-grown 2D sheets were washed using

cyclohexane to remove the residual OA.

Characterization. The grazing incidence X-ray diffraction (GIXRD) analysis was performed using Rigaku Smartlab with CuKα in a θ-2θ scan mode. X-ray photoelectron spectroscopy (XPS) was measured by Thermo scientific Escalab 250Xi. Photoluminescence (PL) and time-resolved photoluminescence (TRPL) spectrum of single crystals were measured with Edinburgh Instruments FLS 980 spectrometer that coupled with optical microscopy. PL mapping of crystal surface was measured with Witec alpha300RA with the excitation source of a 405nm fiber-coupled laser. The UV-visible absorption spectra were recorded under a Hitachi UH4150 spectrometer. Scanning electronic microscope (SEM) and energy-dispersive X-ray (EDS) spectroscopy were performed using a Zeiss Merlin system. High-resolution transmission electron microscopy were observed using a FEI Talos F200X.

Optoelectronic device fabrication and measure. The as-grown 2D $FAPbBr_3$ sheets were placed into the thermal evaporator under the pressure of 1.0×10^{-6} mbar, and a 100 nm of Au electrodes were deposited on the sheet surface with a shadow mask. The devices were illuminated using a semiconductor diode laser CNI MDL-XS-405, and the photocurrents were generated and measured using Keithley 2614B source meter with a probe station. The active device area was about 50 μm estimated by the bias gaps multiplied by the sheet width. The laser power was obtained using an optical power meter (Thorlabs, S121C). The time-dependent photoresponse signal was recorded using a digital oscilloscope (National Instruments, PXI-5122). All experimental measurements were carried out at room temperature.

Results and Discussion

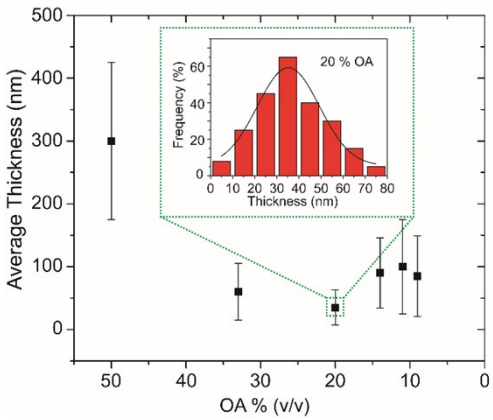

Figure S1 The average thicknesses of 2D $FAPbBr_3$ sheets that grown from the precursor solutions with various OA concentrations (volume percent). The inset is the histogram and distribution of the sheet thicknesses for the 20 % OA solution.

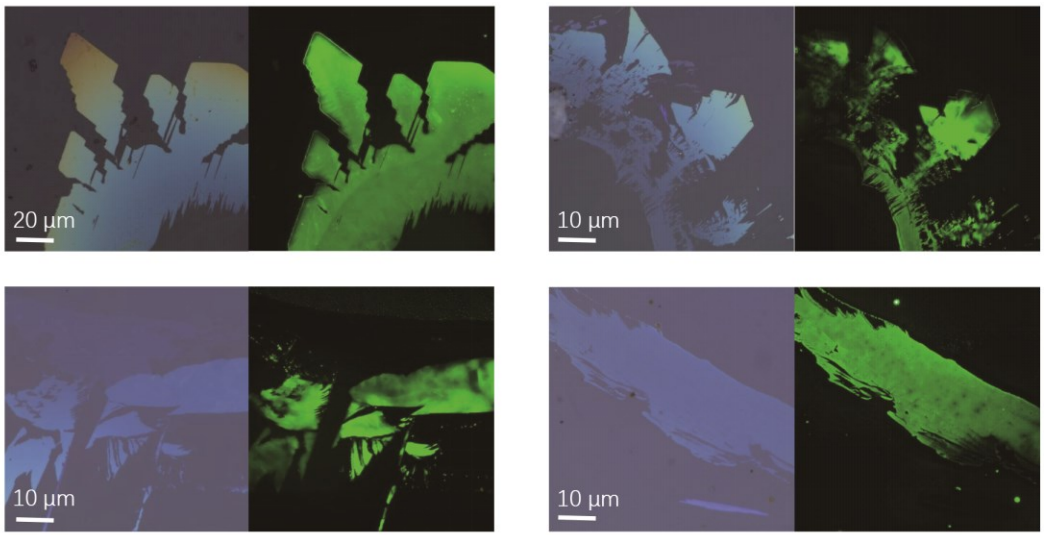

Figure S2 Optic and fluorescent images of 2D $FAPbBr_3$ sheets grown on the mica substrate

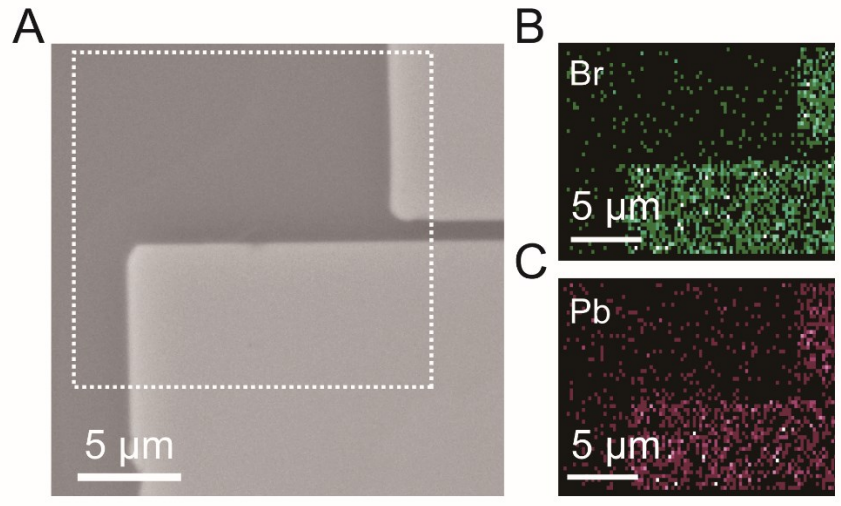

Figure S3 The SEM image (**A**) and EDS element mapping images of Br (**B**) and Pb (**C**) of 2D $FAPbBr_3$ sheets on the mica substate.

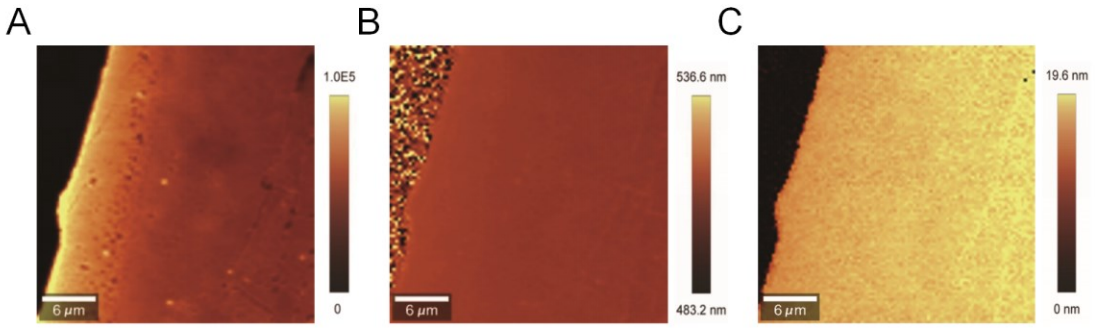

Figure S4 PL emission intensity, peak value, and FWHM distributions of the single-crystalline 2D $FAPbBr_3$ sheet

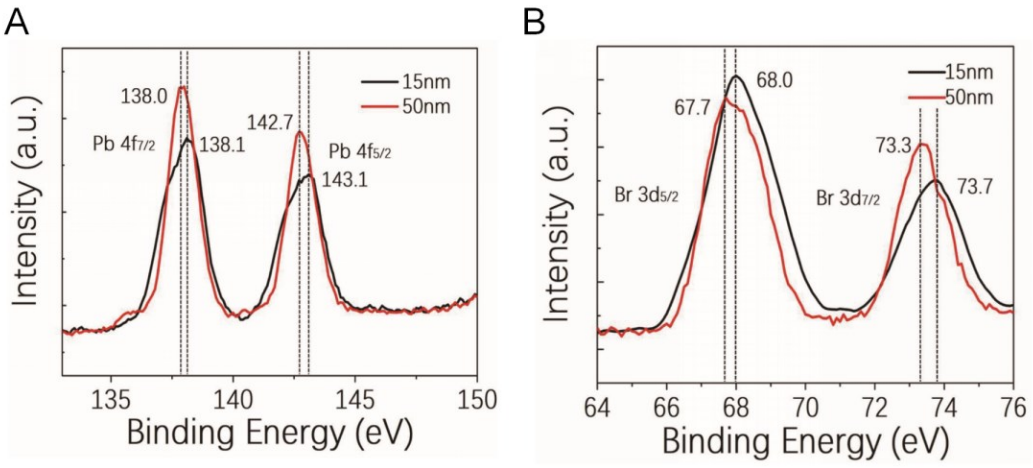

Figure S5 Pb 4f and Br 3d XPS spectra for two single-crystalline 2D $FAPbBr_3$ sheets with the 15 and 50 nm thicknesses, respectively.

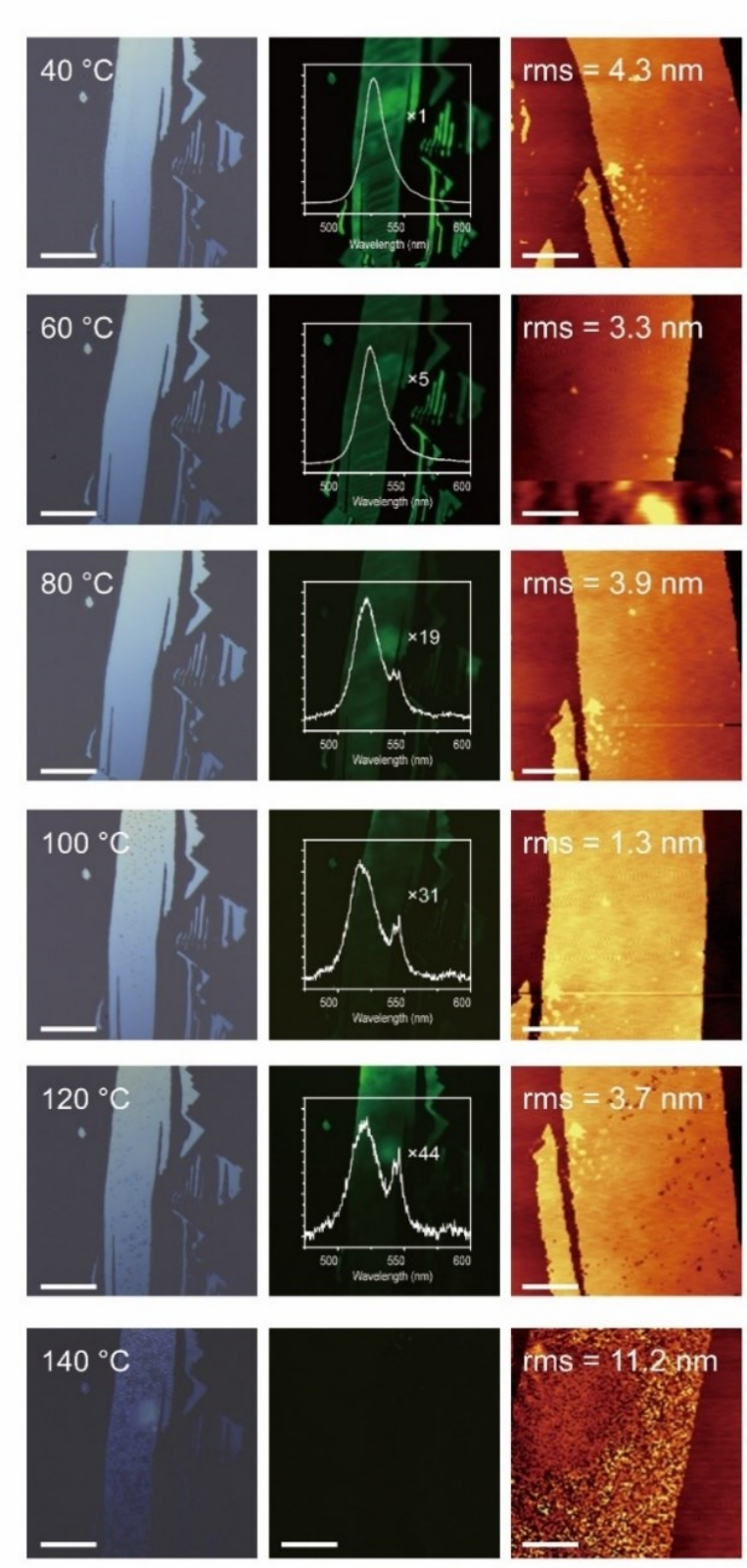

Figure S6 Optic, fluorescent and AFM images of a 25nm-thick $FAPbBr_3$ sheets dependent on the heat temperature. The inset spectra are the PL emissions of 2D sheet.

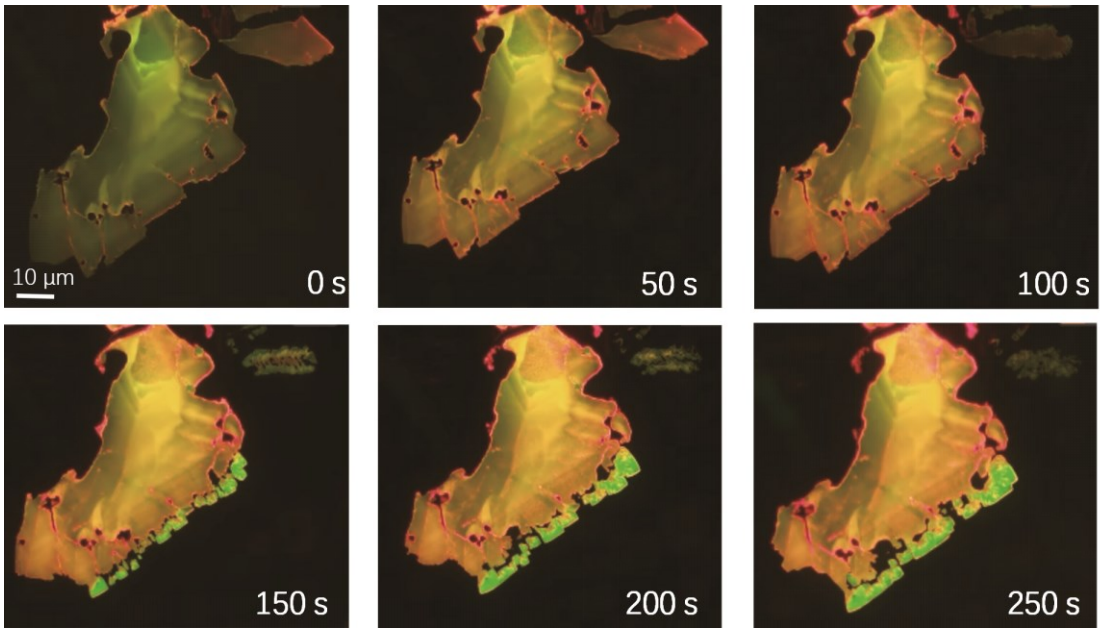

Figure S7 In-situ fluorescent images of photoinduced phase segregation of mixed-halide 2D $FAPb(Br_xI_{1-x})_3$ sheets

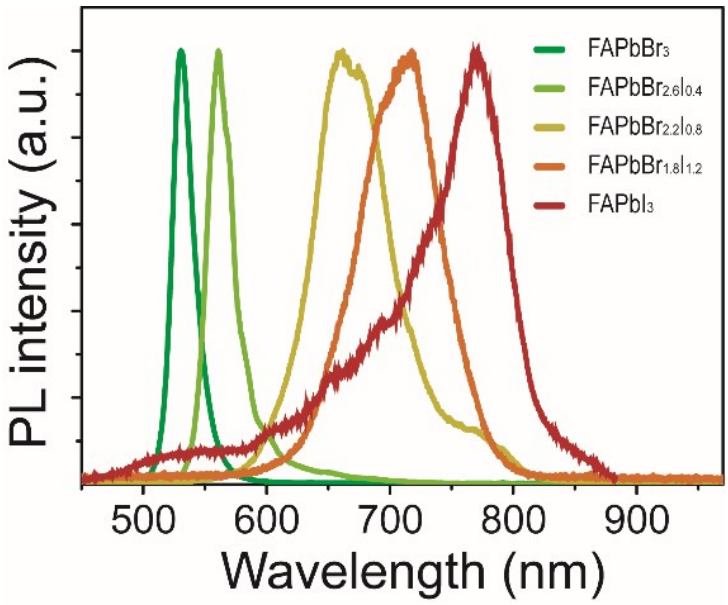

Figure S8 The PL emissions of mixed-halide 2D $FAPb(Br_xI_{1-x})_3$ sheets grown using the liquid-phase epitaxy technique.

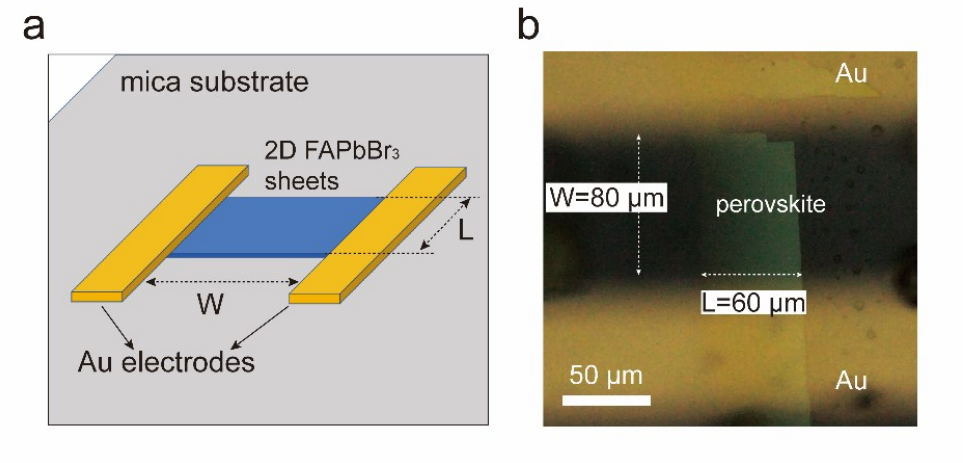

Figure S9 The schematic (**a**) and optical microscope image (**b**) of the in-plane structured device for the SCLC measurements.

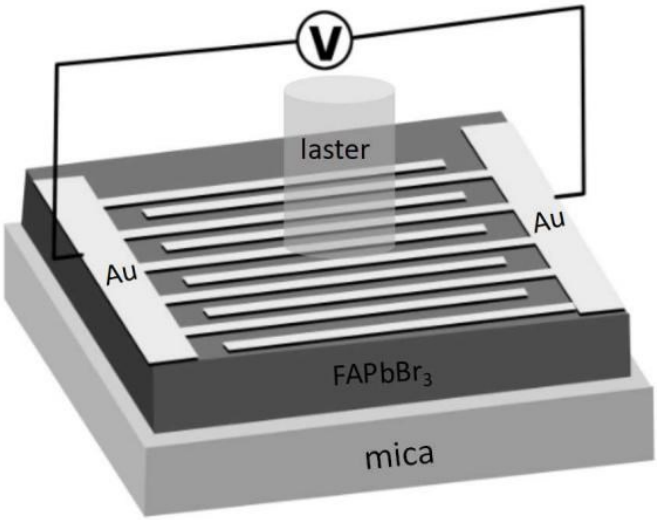

Figure S10 Structure illustration of 2D $FAPbBr_3$-based photodetector.

Table S1 PL emission performance comparisons of $FAPbBr_3$

perovskite	PL (nm)	fwhm (nm)	lifetime (ns)	reference
2D $FAPbBr_3$ single-crystalline sheets	530	20	17~140	this work
$FAPbBr_3$ thin film	534	20.5	89.97	2020[2]
	532	21	46.5	2019[3]
	531.8	24.8		2018[4]
	518	20	13.2	2018[5]
	530	22.6	42.3	2017[6]
	533		24	2017[7]
	528	27	79.63	2017[8]
	530	22	40	2016[9]
	532.1	26.2	10.2	2016[10]
$FAPbBr_3$ bulk single crystal	567		282±5	2018[11]
	577.5		72000	2017[12]
	587		2272	2016[13]

Table S2 Summary of photodetector performances basing on $FAPbBr_3$ perovskites

Active material	n_{trap} (cm^{-3})	Responsivity (A/W)	τ_{raise}/τ_{fall} (ms)	Mobility ($cm^2V^{-1}S^{-1}$)	Diffusion length (μm)	reference
2D $FAPbBr_3$ single-crystalline sheets	2.58×10^{11}	730	0.67/0.7	31	1.2	this work
$(OA)2FA_{n-1}Pb_nBr_{3n+1}$ micro-platelets	-	32	0.25/1.45	-	-	2017[14]
$FAPbBr_3$ microcrystals	6.98×10^{11}	4000	0.67/0.75	-	-	2018[11]
$FAPbBr_3$ nanoparticles	-	8	2600/300	-	-	2020[15]
$FAPbBr_3$ bulk single crystals	9.60×10^{9}	-	-	62±11	19	2016[13]
	-	-	-	14±2	1.3	2015[16]

References

1. Y. Bai, H. X. Zhang, M. J. Zhang, D. Wang, H. Zeng, H. Xue, W. Z. Wu, Y. Xie, Y. X. Zhang, H. Jing, J. Su, H. H. Yu, Z. G. Hu, R. W. Peng, Y. C. Wu, *Nanoscale*, 2020, **12**, 1100.
2. Y. Q. Zu, J. Xi, L. Li, J. F. Dai, S. P. Wang, F. Yun, B. Jiao, H. Dong, X. Hou, Z. X. Wu, *ACS Appl. Mater. Interfaces*, 2020, **12**, 2835-2841.

3. H. Fang, W. Deng, X. J. Zhang, X. Z. Xu, M. Zhang, J. S. Jie, X. H. Zhang, *Nano Research*, 2019, **12**, 171-176.
4. D. Yu, F. Cao, Y. Gao, Y. Xiong, H. Zeng, *Adv. Funct. Mater.*, 2018, **28**, 1800248.
5. Y.-L. Tong, Y.-W. Zhang, K. Ma, R. Cheng, F. Wang, S. Chen, *ACS Appl. Mater. Interfaces*, 2018, **10**, 31603-31609.
6. S. Kumar, J. Jagielski, N. Kallikounis, Y.-H. Kim, C. Wolf, F. Jenny, T. Tian, C. J. Hofer, Y.-C. Chiu, W. J. Stark, T.-W. Lee, C.-J, Shih, *Nano Lett.*, 2017, **17**, 5277-5284.
7. I. Levchuk, A. Osvet, X. Tang, M. Brandl, J. D. Perea, F. Hoegl, G. J. Matt, R. Hock, M. Batentschuk, C. J. Brabec, *Nano Lett.*, 2017, **17**, 2765-2770.
8. Y.-H. Kim, G.-H. Lee, Y.-T. Kim, C. Wolf, H. J. Yun, W. Kwon, C. G. Park, T.-W. Lee, *Nano Energy*, 2017, **38**, 51-58.
9. L. Protesescu, S. Yakunin, M. I. Bodnarchuk, F. Bertolotti, N. Masciocchi, A. Guagliardi, M. V. Kovalenko, *J. Am. Chem. Soc.*, 2016, **138**, 14202-14205.
10. A. Perumal, S. Shendre, M. Li, Y. K. Tay, V. K. Sharma, S. Chen, Z. Wei, Q. Liu, Y. Gao, P. J. Buenconsejo, S. T. Tan, C. L. Gan, Q. Xiong, T. C. Sum, H. V. Demir, *Sci. Rep.*, 2016, **6**, 36733.
11. F. Y. Zhang, B. Yang, K. B. Zheng, S. Q. Yang, Y. J. Li, W. Q. Deng, R. X. He, *Nano-Micro Lett.*, 2018, **10**, 43.
12. E. Alarousu, A.M. El-Zohry, J. Yin, A. A. Zhumekenov, C. Yang, E. Alhabshi, L. Gereige, A. AlSaggaf, A. V. Malko, O. M. Bakr, O. F. Mohammed, *J. Phys. Chem. Lett.*, 2017, **8**, 4386-4390.
13. A. A. Zhumekenov, M. I. Saidaminov, M. A. Haque, E. Alarousu, S. P. Sarmah, B. Murali, I. Dursun, X.-H. Miao, A. L. Abdelhady, T. Wu, O. F. Mohammed, O. M. Bakr, *ACS Energy Let.*, 2016, **1**, 32-37.
14. D. J. Yu, F.Cao, Y.L.Shen, X.H. Liu, Y. Zhu, H.B. Zeng. *J. Phys. Chem. Lett*, 2017, **8**, 2565-2572.
15. S. K. Si, S. Paria, S. K. Karan, S. Ojha, A. K. Das, A. Maitra, A. Bera, L. Halder, A. De, B. B. Khatua, *Nanoscale*, 2020, **12**, 7214-7230.
16. W. Rehman, R. L. Milot, G.E. Eperon, C.Wehrenfenning, J. L. Boland, H. J. Snaith, M.b. Johnston, L.M. Herz. *Advance Materials*, 2015, **27**, 7938-7944.